

Journal of
Astronomical Telescopes,
Instruments, and Systems

AstronomicalTelescopes.SPIEDigitalLibrary.org

**Edgewise connectivity: an approach
to improving segmented primary
mirror performance**

Jessica Gersh-Range
William R. Arnold, Sr.
H. Philip Stahl

Edgewise connectivity: an approach to improving segmented primary mirror performance

Jessica Gersh-Range,^{a,*} William R. Arnold Sr.,^b and H. Philip Stahl^c

^aCornell University, 127 Upson Hall, Ithaca, New York 14853, United States

^bDefense Acquisition, Inc., Jacobs ESSSA Group, Huntsville, Alabama 35806, United States

^cNASA Marshall Space Flight Center, Huntsville, Alabama 35812, United States

Abstract. As future astrophysics missions require space telescopes with greater sensitivity and angular resolution, the corresponding increase in the primary mirror diameter presents numerous challenges. Since fairing restrictions limit the maximum diameter of monolithic and deployable segmented mirrors that can be launched, there is a need for on-orbit assembly methods that decouple the mirror diameter from the choice of launch vehicle. In addition, larger mirrors are more susceptible to vibrations and are typically so lightly damped that vibrations could persist for some time if uncontrolled. To address these challenges, we present a segmented mirror architecture in which the segments are connected edgewise by mechanisms analogous to damped springs. These mechanisms can be damped springs, flux-pinning mechanisms, virtual mechanisms, or any other device with the same basic behavior. Using a parametric finite-element model, we show that for low to intermediate stiffnesses, the stiffness and damping contributions from the mechanisms improve both the natural frequency and disturbance response of the segmented mirror. At higher stiffnesses, the mechanisms structurally connect the segments, leading to a segmented mirror that performs comparably to a monolith—or better, depending on the mechanism damping—with the modular design enabling on-orbit assembly and scalability.

© The Authors. Published by SPIE under a Creative Commons Attribution 3.0 Unported License. Distribution or reproduction of this work in whole or in part requires full attribution of the original publication, including its DOI. [DOI: [10.1117/1.JATIS.1.1.014002](https://doi.org/10.1117/1.JATIS.1.1.014002)]

Keywords: segmented mirror; edgewise connectivity; space telescope; flexibility; stiffness; damping; vibration; disturbance response.

Paper 14002P received Mar. 3, 2014; revised manuscript received Jun. 10, 2014; accepted for publication Jul. 25, 2014; published online Oct. 24, 2014.

1 Introduction

As future astrophysics missions require space telescopes with greater sensitivity and angular resolution, the corresponding increase in the primary mirror diameter presents numerous design challenges. Some of these challenges, such as packaging and deployment, are related to the choice of launch vehicle. Since fairing restrictions determine the maximum diameter of a monolithic mirror that can be launched, larger primaries must be segmented and either deployed or assembled on orbit. The 6.6-m primary for the James Webb Space Telescope, for example, consists of 18 segments mounted on a backplane that folds to satisfy the constraints of its 4.57-m-diameter shroud.^{1,2} While scaling this approach and developing more sophisticated packaging strategies may enable launching even larger future observatories,^{3,4} an upper limit on the mirror diameter remains. Ultimately, there is a need for on-orbit assembly techniques that decouple the diameter from the choice of launch vehicle. Proposed methods include formation flight and electromagnetic formation flight, which treat the mirror as an array of free-floating segments and use active control to prevent collisions and maintain optical alignment.^{5–7}

Additional challenges are related to the mirror itself. The image quality, for example, depends on the stability of the mirror surface. In order to take science data, the surface error must remain below a specified tolerance even in the presence of vibrations, which can be excited by thermal snap-

motion of an internal spacecraft mechanism, or the reaction wheels.^{8–10} However, larger mirrors are not only more susceptible to vibrations, but they are also so lightly damped that the vibrations could persist for some time in the absence of control. Since the mirror flexibility scales as D^4/h^2 , where D is the mirror diameter and h is the mirror thickness, the natural frequency is proportional to h/D^2 , and the damping is close to pure material damping, with a damping ratio on the order of 0.01.^{9,11} Methods for stiffening the mirror include increasing the thickness, which may not be possible if the additional mass conflicts with the launch vehicle restrictions, and embedding actuators in the mirror substrate.^{12,13}

To address these challenges, we present a segmented mirror architecture in which the segments are connected edgewise by mechanisms analogous to damped springs, as shown in Fig. 1. To compare the performance of this segmented mirror to that of a monolith with the same size and shape, we have developed a parametric finite-element model that calculates the mode shapes, natural frequencies, and disturbance response for either mirror, as outlined in Sec. 2. Using this tool, we show that the mechanisms can serve one of two functions: structurally connecting the segments or providing supplemental stiffness and damping (Secs. 3 and 4). The particular application is determined by the mechanism stiffness, which affects the mirror at the segment level as well as globally (Sec. 3). For low to intermediate stiffnesses, the stiffness and damping contributions from the mechanisms improve both the natural frequency and the disturbance response of the segmented mirror. At higher stiffnesses, the mechanisms structurally connect the segments, leading to a segmented mirror that performs comparably to

*Address all correspondence to: Jessica Gersh-Range, E-mail: jag389@cornell.edu

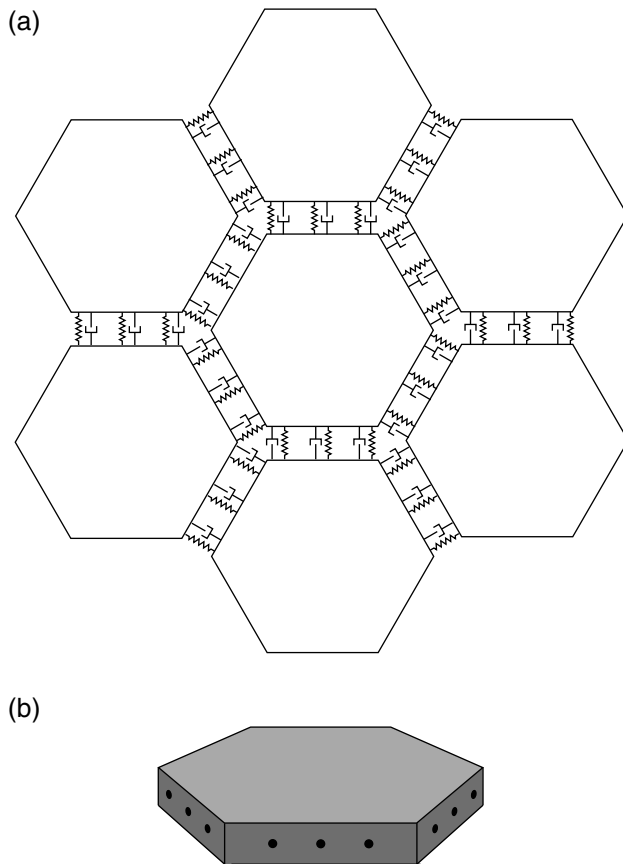


Fig. 1 The edgewise-connected mirror. In this architecture, neighboring segments are connected by mechanisms analogous to damped springs, shown as spring-damper pairs in (a). These mechanisms are installed along the segment edges, as represented by dots in (b), and can consist of actual springs and dampers, flux-pinning mechanisms, or any other device with the same behavior. While the segments could be mounted to a backplane in addition, the question of segmented mirror mount design is beyond the scope of this paper.

or better than the monolith depending on the amount of damping, with the modular design enabling on-orbit assembly and scalability (Sec. 4).

2 Mirror Model

To evaluate the performance of an edgewise-connected mirror, we consider the first natural frequency, which is directly related to the overall mirror stiffness, and the impulse response, which provides insights into the mirror stability. Since the performance is affected by the mirror geometry, mechanism properties, and mechanism placement, we have developed a parametric finite-element model in order to investigate how the mirror design affects the performance. As a basis for comparison, we consider the performance of a monolith of the same size and shape.

The finite-element model consists of submodels for the mirror, mount, and mechanisms. In the mirror model, a basic mirror is composed of rings of hexagonal segments and can be either segmented or monolithic depending on how these segments are connected. For an edgewise-connected mirror, the segments are separated by a gap, and the edges of adjacent segments are connected at discrete locations by a collection of damped spring elements that represent the mechanisms [Fig. 2(b)]. For a monolithic mirror, there is no gap between the segments, and the edges of adjacent segments are connected continuously by merging the coincident nodes [Fig. 2(a)]. A specific mirror model is generated using a set of geometric parameters that includes the mirror diameter D , the size of the gap between the segments, the number of rings n_r , the mirror curvature, and the aspect ratio. For an edgewise-connected mirror, the number of mechanisms n_e along each edge, the mechanism placement, and the mechanism properties are additional parameters.

For simplicity and consistency, the monolithic and edgewise-connected mirrors are mounted identically, and the mount model consists of two options: the mirror as a whole is either entirely unsupported or kinematically mounted at three edge nodes spaced by 120 deg. While each segment of an edgewise-connected mirror could be mounted on a backplane in addition

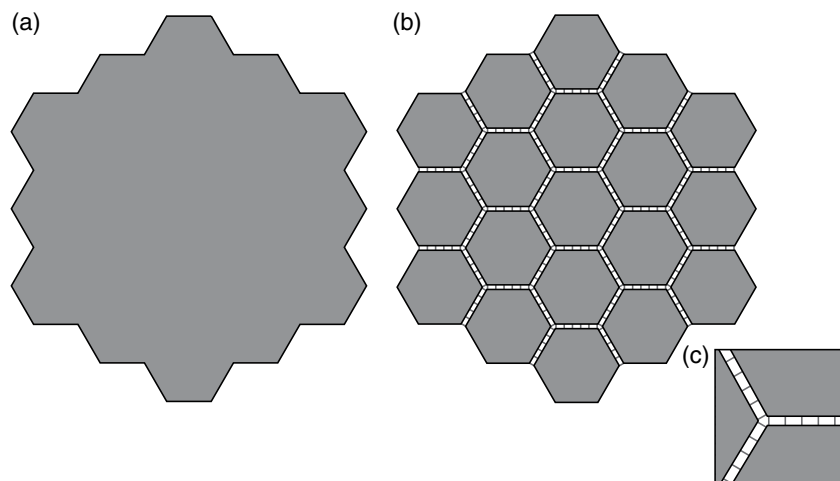


Fig. 2 Mirror modeling. In the finite-element model, a mirror is composed of rings of hexagonal segments, with the connectivity determining whether the mirror is monolithic or segmented. For a monolithic mirror (a), the segments are connected continuously along the edges, while for an edgewise-connected mirror (b), the segments are connected at discrete locations by collections of damped springs that represent the mechanisms (c).

to being connected edgewise, the problem of segmented mirror mount design is beyond the scope of this paper.

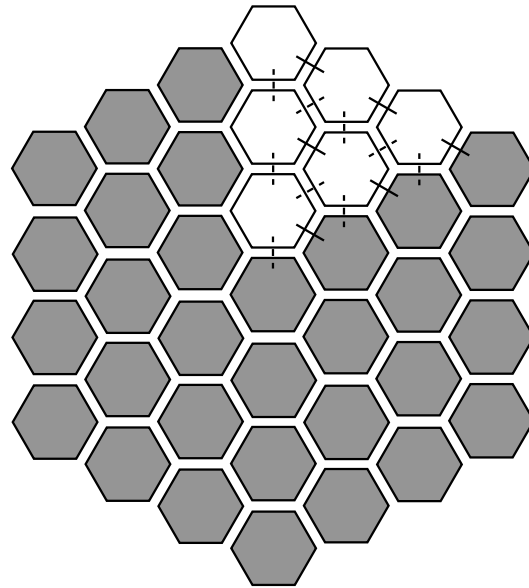
The mechanism model represents each mechanism as a collection of damped springs. As an example, we consider a case in which all of the important dynamics can be captured using four collocated single-degree-of-freedom damped springs. Three of these damped springs correspond to translations parallel and perpendicular to the mirror edge, with the fourth corresponding to bending. It is assumed that while the damping is isotropic, the stiffness is not: the stiffness for perpendicular translation, k_{\perp} , is twice that for parallel translation, k_{\parallel} , and directly proportional to the bending stiffness, k_b . This particular mechanism model can be used to describe flux-pinning mechanisms,¹⁴ an actual collection of damped springs, or any other mechanism with the same behavior. The model also applies to the case of virtual mechanisms, in which sensors detect the relative motion between segments, actuators resist or correct this motion, and a control algorithm determines the appropriate actuator response.

In the simulations that follow, we consider a baseline 15-m mirror with two rings of segments, six mechanisms per edge, and an aspect ratio of 100, and we vary individual design parameters to determine their effects on the mirror performance. The choice of a 15-m mirror is driven by the AURA “Beyond JWST” study, which is determining aperture requirements for the next generation of space telescopes. Preliminary results indicate that while the minimum acceptable aperture diameter is 6.5 to 8 m, an aperture of 12 to 14 m is desired, and a 16-m aperture is highly desirable.¹⁵ Since the natural frequency is directly proportional to the mirror thickness, we consider aspect ratios from 80 to 120; this range is expected to cover the spectrum of conservatively thick to aggressively thin designs.¹⁶ To examine the importance of the mechanism stiffness, we consider k_{\perp} values ranging from 10 to 10^9 N/m. At the upper end of this range, k_b is comparable to the approximate plate constant, the bending stiffness of a circular plate with the same diameter and material properties as the monolithic mirror. The limiting case of infinitely stiff mechanisms is also considered by using the CERIG command in ANSYS¹⁷ to rigidly connect the nodes defining the spring elements. Similarly, to examine the importance of the mechanism damping, we consider values ranging from 0 to 10^6 kg/s.

Since the total stiffness and damping contributions from the mechanisms depend on the total number of mechanisms N_{mech} in addition to the individual mechanism properties, we also consider parameters that affect this number. In the edgewise-connected mirror, the total number of mechanisms depends on the number of mechanisms n_e along each edge as well as the number of edge connections. There are two types of edge connections: connections between segments in the same ring and connections between segments in neighboring rings. As illustrated in Fig. 3, for the i th ring, there are $6i$ sets of edge connections within the ring and $6(2i - 1)$ sets of connections to ring $i - 1$. As a result, there are $9n_r^2 + 3n_r$ sets of edge connections within the entire mirror, and the total number of mechanisms is given by

$$N_{\text{mech}} = n_e(9n_r^2 + 3n_r). \quad (1)$$

Since the total number of mechanisms depends on n_e , we consider 3 to 8 mechanisms per edge. Similarly, since the total number depends on n_r , we consider 1 to 4 rings; these ring numbers correspond to segments that are between 1 and



Ring number	1	2	3	i
— Sets of edge connections within a ring	6(1)	6(2)	6(3)	$6(i)$
- - - Sets of edge connections to the previous ring	6(1)	6(3)	6(5)	$6(2i-1)$

Fig. 3 Mechanism totals by ring number. The total number of mechanisms depends on the number of mechanisms used to connect a pair of adjacent edges, n_e , as well as the number of edge pairs. For ease of counting, the edge pairs are divided into two categories: in-ring pairs, for segments in the same ring, and cross-ring pairs, for segments in rings i and $i - 1$. For a mirror with n_r rings, there are $9n_r^2 + 3n_r$ pairs, for a total of $n_e(9n_r^2 + 3n_r)$ mechanisms.

5 m flat to flat, a range that includes sizes within current manufacturing capabilities as well as sizes that require technology development.⁵

3 Relating Mirror Motions to Mechanism Applications

When mirror segments are connected edgewise by springlike mechanisms, the overall stiffness along the segment edges affects the mirror behavior both globally and at the segment level. The edge stiffness is determined by the mechanism stiffness and the number of mechanisms along each edge, and it influences the first natural frequency as well as the motion of the segments, which can move as a unit or as individual rigid bodies. These different segment motions correspond to different mechanism applications: for sufficiently high edge stiffnesses, the mechanisms serve as structural attachments between the segments, with the segments moving as a cohesive unit. For lower edge stiffnesses, the mechanisms provide supplemental stiffness and damping even if the segments move as individual rigid bodies. To understand the conditions under which the mechanisms are suited for each purpose, we have conducted a series of parameter studies that investigate the relationship between the edgewise-connected mirror design and the resulting behavior.

The edge stiffness is affected by two main factors: the number of connections between adjacent mirror segments and the equivalent stiffness of all the mechanisms along the edge.

These factors are controlled by two of the design parameters, the number of mechanisms along an edge and the mechanism stiffness, but they are not always adjusted independently. While the number of connections is directly related to the number of mechanisms, adding a mechanism also increases the equivalent stiffness. (Note that the mechanisms along a segment edge correspond to sets of springs in parallel, so for a given degree of freedom, the equivalent stiffness is directly proportional to both the mechanism stiffness and n_e .) However, the effect that increasing the connectivity has on the mirror behavior can be isolated by considering the case of infinitely stiff mechanisms since in this limit adding mechanisms increases the number of connections without affecting the equivalent stiffness. Similarly, the effect of increasing the equivalent stiffness can be isolated by fixing the number of mechanisms and varying the mechanism stiffness.

As Fig. 4 shows, the equivalent stiffness is the dominant factor in determining the global mirror behavior. Although replacing the continuously connected edges of the monolith with discretely connected edges lowers the natural frequency, the effect is minimal. Even with as few as three mechanisms per edge, the frequency in the infinite-stiffness case is within

4% of the monolithic value, and it asymptotes to the monolithic value as the number of mechanisms increases. This asymptotic behavior is to be expected since the discrete connectivity approaches continuity in the limit of infinitely many mechanisms per edge. By comparison, decreasing the mechanism stiffness can decrease the frequency by orders of magnitude, and as expected, increasing the number of mechanisms increases the frequency. The same trends are observed whether the mirror is conservatively thick or aggressively thin.

One particularly significant result is that the frequency curves cluster as k_b approaches the approximate plate constant. As shown in Fig. 5, a plot of the frequency as a function of mechanism stiffness divides into three regions. In the low- and intermediate-stiffness regions, the frequency increases as approximately the square root of the stiffness, but in the high-stiffness region, the increase is much slower. This result suggests that while aggressively increasing the bending stiffness may be beneficial in the low- and intermediate-stiffness regimes, it may not be worthwhile in the high-stiffness regime, especially if significant cost is involved.

The transitions from one stiffness regime to the next correspond to changes in the segment motion, as evidenced by

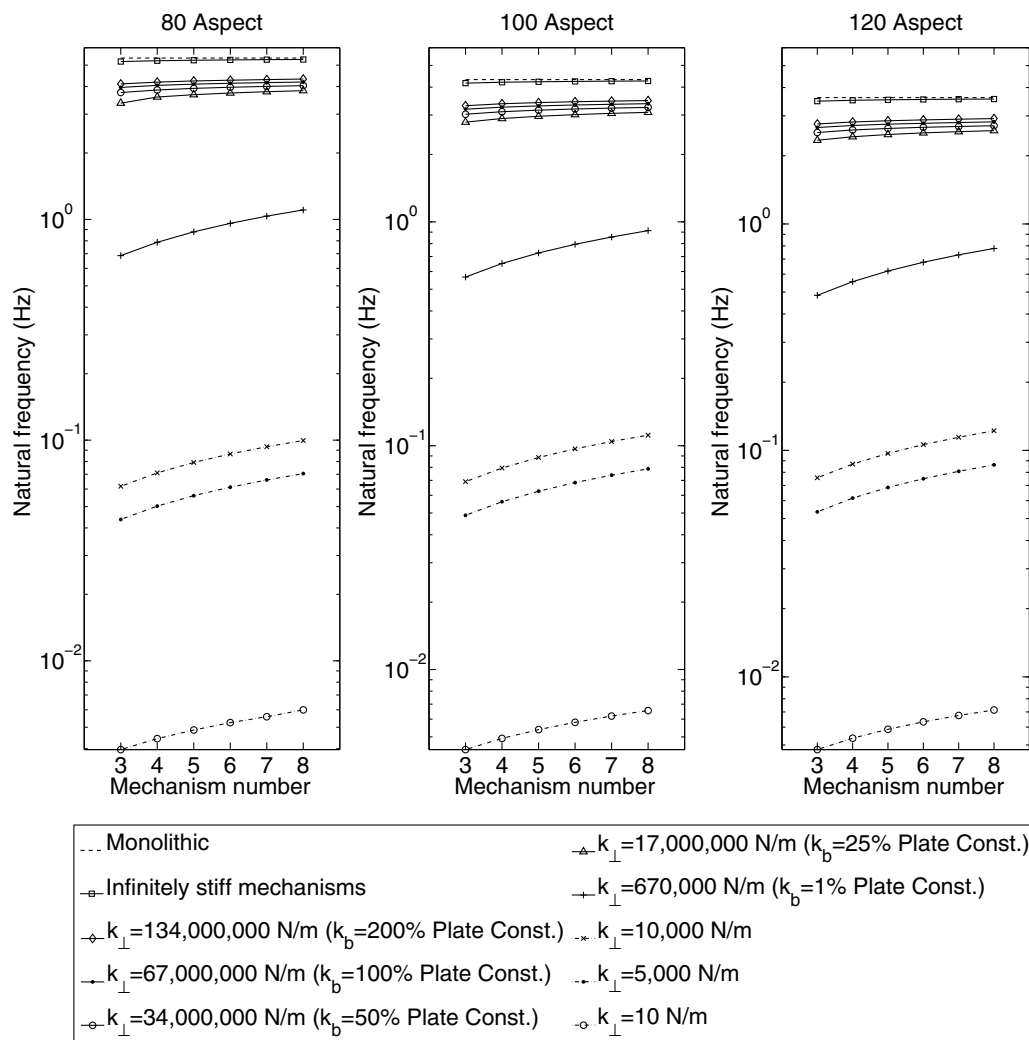


Fig. 4 The first natural frequency as a function of aspect ratio, mechanism number, and mechanism stiffness.

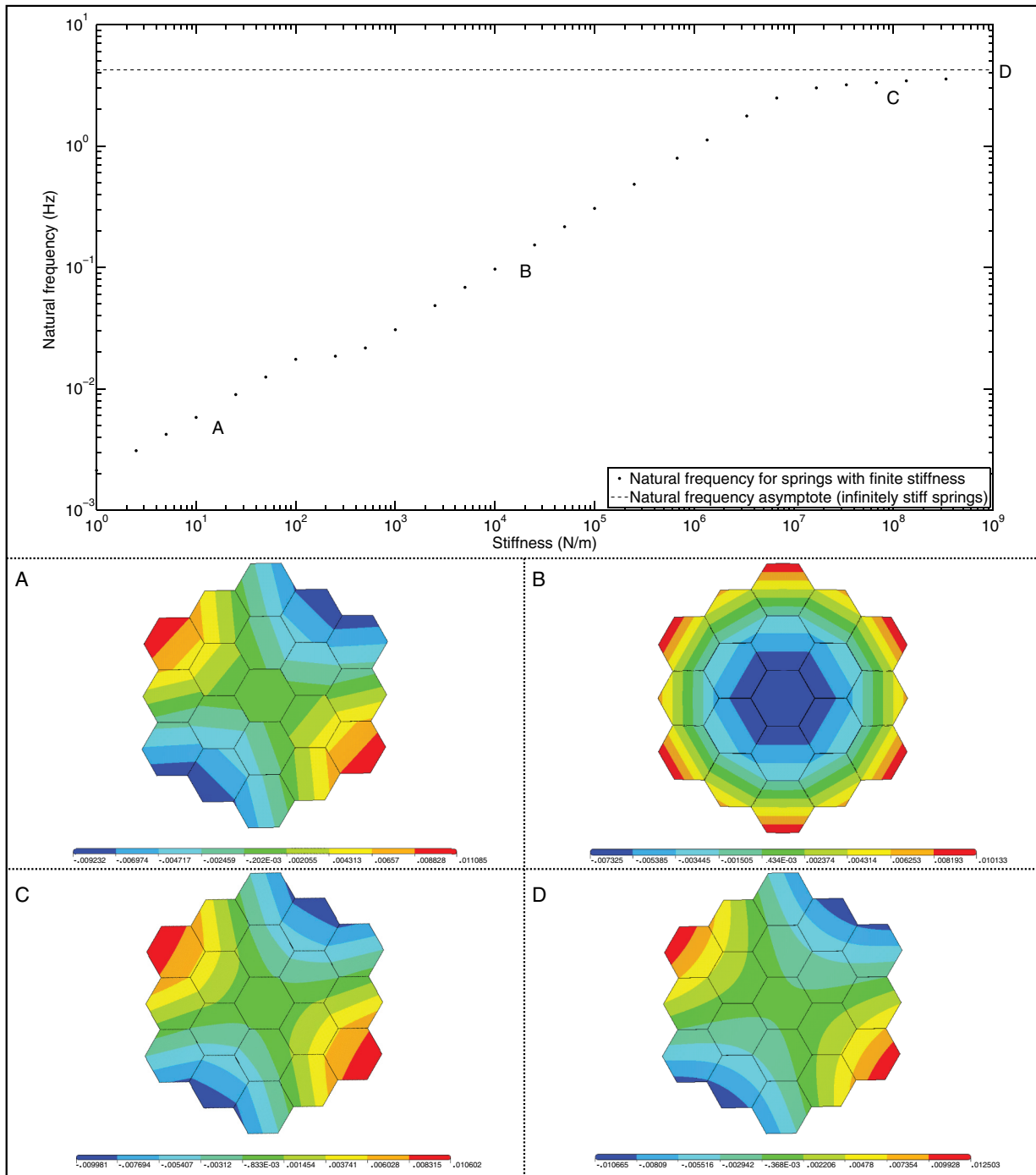


Fig. 5 Mechanism stiffness regimes and the corresponding segment motion. The mechanism stiffness affects the mirror behavior globally and at the segment level. For low-stiffness mechanisms (A), the segments conform to the mode shape by tilting as individual rigid bodies. For intermediate-stiffness mechanisms (B), the segments start to move as a unit while still tilting as individual rigid bodies. In these cases, the mechanisms are a source of supplemental stiffness and damping, and the natural frequency is approximately proportional to the square root of the mechanism stiffness. For high-stiffness mechanisms (C), the segments bend as a cohesive unit, indicating that the mechanisms serve as structural attachments between the segments. In this regime, increasing the mechanism stiffness has a minimal effect on the natural frequency. The limiting case of infinitely stiff mechanisms (D) is shown for reference.

changes in the mode shapes. In the low-stiffness regime, the mode shape contours are straight across the segments and discontinuous across the segment boundaries, which indicates that the segments conform to the mode shape by tilting as individual rigid bodies. In the high-stiffness regime, the contours

curve within a segment and are continuous across the boundaries, indicating that the segments bend as a single, cohesive unit. In this regime, the mechanisms are strong enough that the bending stiffness along the segment edges is comparable to the bending stiffness of the monolithic mirror, and as a result,

the edgewise-connected mirror behaves similarly to the monolith. In between these cases, in the intermediate-stiffness regime, the contours are straight across the segments and the mode shape has shifted so that the contours are continuous across the segment boundaries. In this case, the segments move as a unit while still tilting as individual rigid bodies. These results suggest that the mechanisms function as structural attachments in the high-stiffness regime and as supplemental sources of stiffness and damping in the low- and intermediate-stiffness regimes.

4 Mirror Performance Studies

One important performance metric for a primary mirror is the settling time required after disturbances induce vibration. Since the mirror surface error must remain below a specified limit during science observations, time spent excessively vibrating reduces the observatory efficiency. To evaluate the performance of an edgewise-connected mirror relative to its equivalent monolith, we consider the time history of the root-mean-square surface error after an impulse disturbance is applied to one of the supports. This type of disturbance could arise from thermal snap, as seen on Hubble,^{8,9} or other sources, including motions of internal spacecraft mechanisms such as tape recorders or filter wheels.^{9,10}

For the edgewise-connected mirror, the disturbance response depends on the total stiffness and damping contributions from the mechanisms. These contributions are affected by both the individual mechanism properties and the total number of mechanisms. While the total number of mechanisms can be adjusted by changing either the number of mechanisms n_e along each edge or the number of rings n_r , only the number of rings will be considered since the mechanism number increases quadratically with n_r but only linearly with n_e , as shown in Eq. (1).

The mechanism stiffness primarily affects the response by determining the strength of the connections between the segments. For high-stiffness mechanisms, which serve as structural attachments, the connections are strong enough for the segments to move as a unit, while for lower-stiffness mechanisms, the connections can be much weaker. The difference in connection

strength translates into a difference in the ease with which disturbances propagate across the mirror surface, with stronger connections corresponding to increased propagation. As a result, higher stiffnesses lead to larger disturbance responses, as shown in Fig. 6.

Since the stiffness affects the disturbance propagation, mechanisms that serve as structural attachments have different response characteristics than mechanisms that serve as supplemental sources of stiffness and damping. To examine these differences, we consider mechanisms for each application, with high-stiffness mechanisms representing the structural application and intermediate-stiffness mechanisms representing the supplemental application. As shown in Fig. 7, four basic responses are possible. With high-stiffness mechanisms, the edgewise-connected mirror has a disturbance response comparable to or better than that of the monolith. In the low-damping case, the response oscillates with approximately the same magnitude and minimal decay, and in the high-damping case, the response improves noticeably, oscillating at a single frequency and decaying by nearly an order of magnitude in only 5 s. With intermediate-stiffness mechanisms, the edgewise-connected mirror has a response at least an order of magnitude lower than that of the monolith due to the decreased disturbance propagation. In the low-damping case, the response varies little over 5 s, while in the high-damping case, the response decays rapidly, decreasing by several orders of magnitude.

While increasing the mechanism damping generally increases the decay rate, the amount of change depends on the mechanism stiffness. Since disturbances propagate less effectively in the intermediate-stiffness cases, increasing the damping has a more pronounced effect [Fig. 8(a)]. With very high damping, the dampers also begin to connect the segments. In Fig. 8, the optimal damping for the intermediate-stiffness mechanisms is on the order of 100,000 kg/s since the resulting response has the quickest decay without any oscillation. With additional damping, the response has a larger initial transient and oscillates with an amplitude comparable to that of the monolith response, indicating that the dampers are connecting the segments. In the high-stiffness cases, the increased connection strength is less

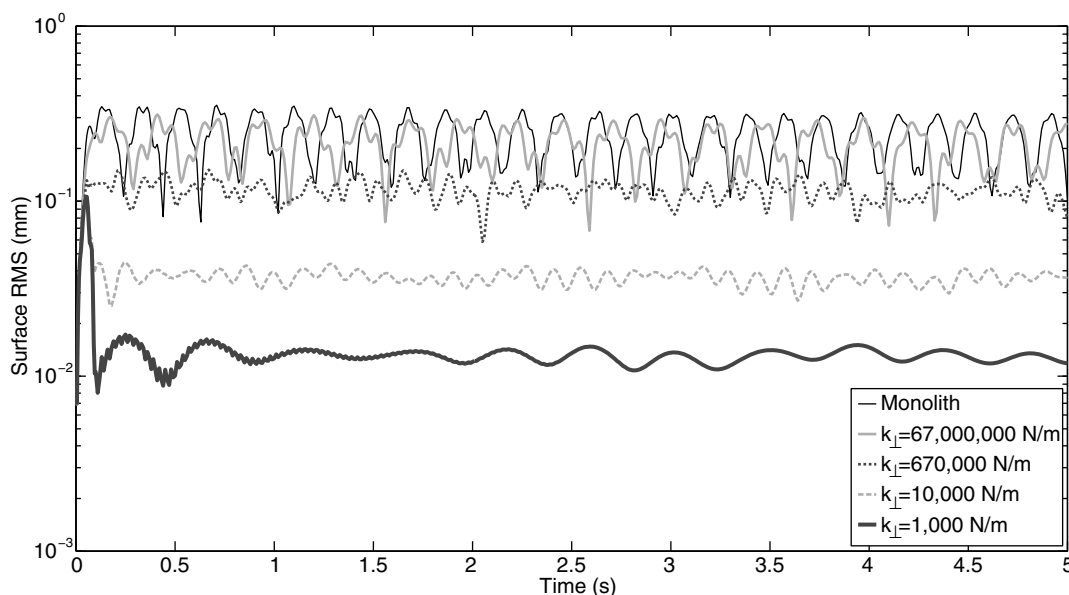


Fig. 6 The effects of mechanism stiffness on the impulse response.

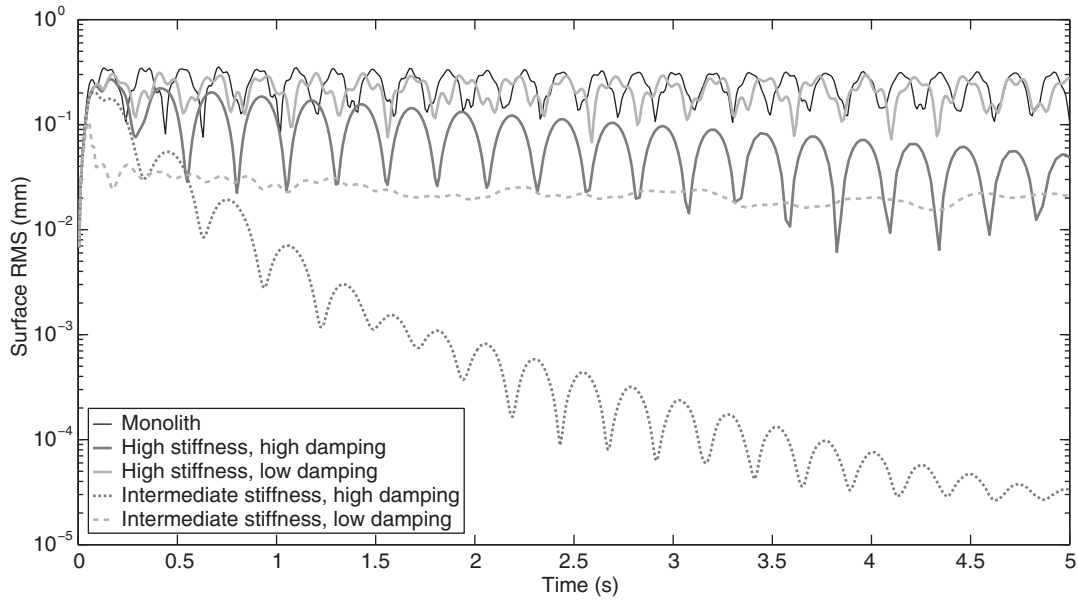


Fig. 7 Limiting cases for the impulse response.

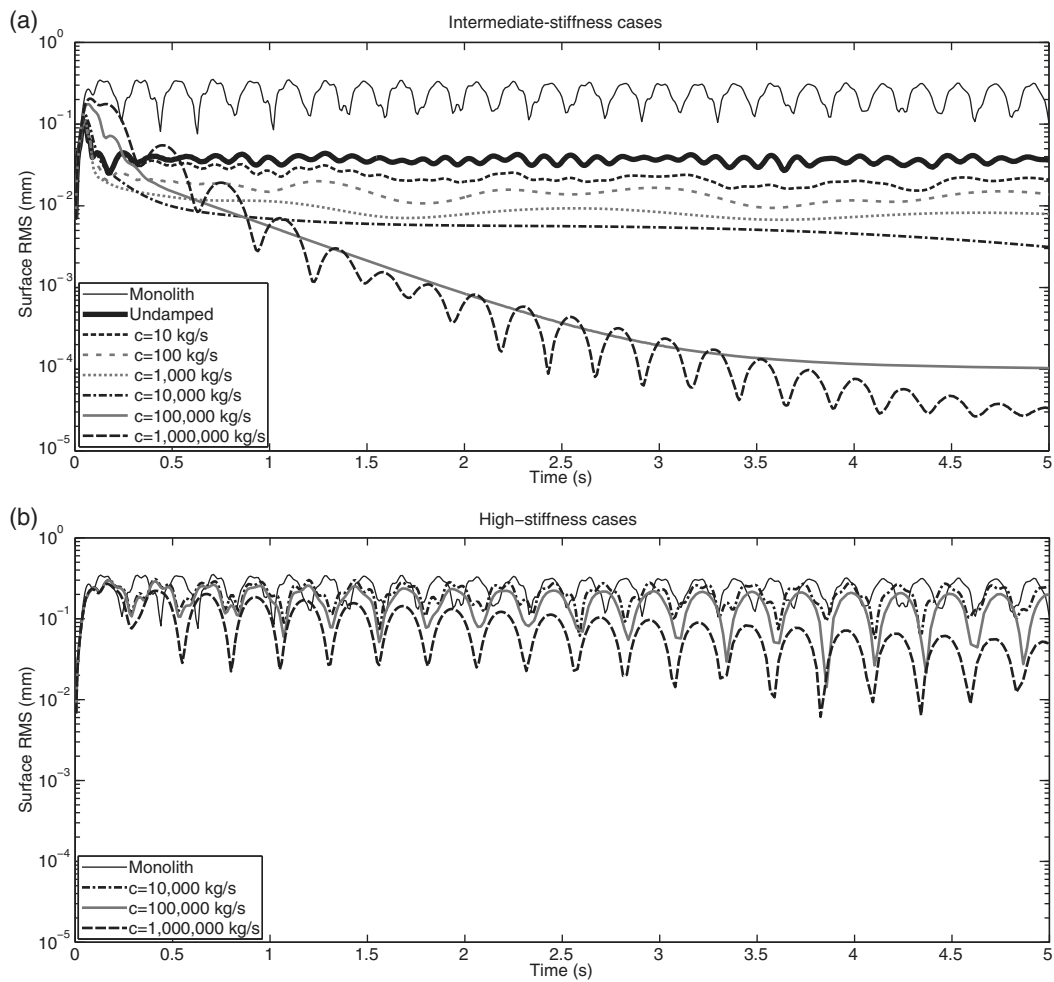


Fig. 8 The effects of damping on the impulse response for (a) intermediate- and (b) high-stiffness mechanisms.

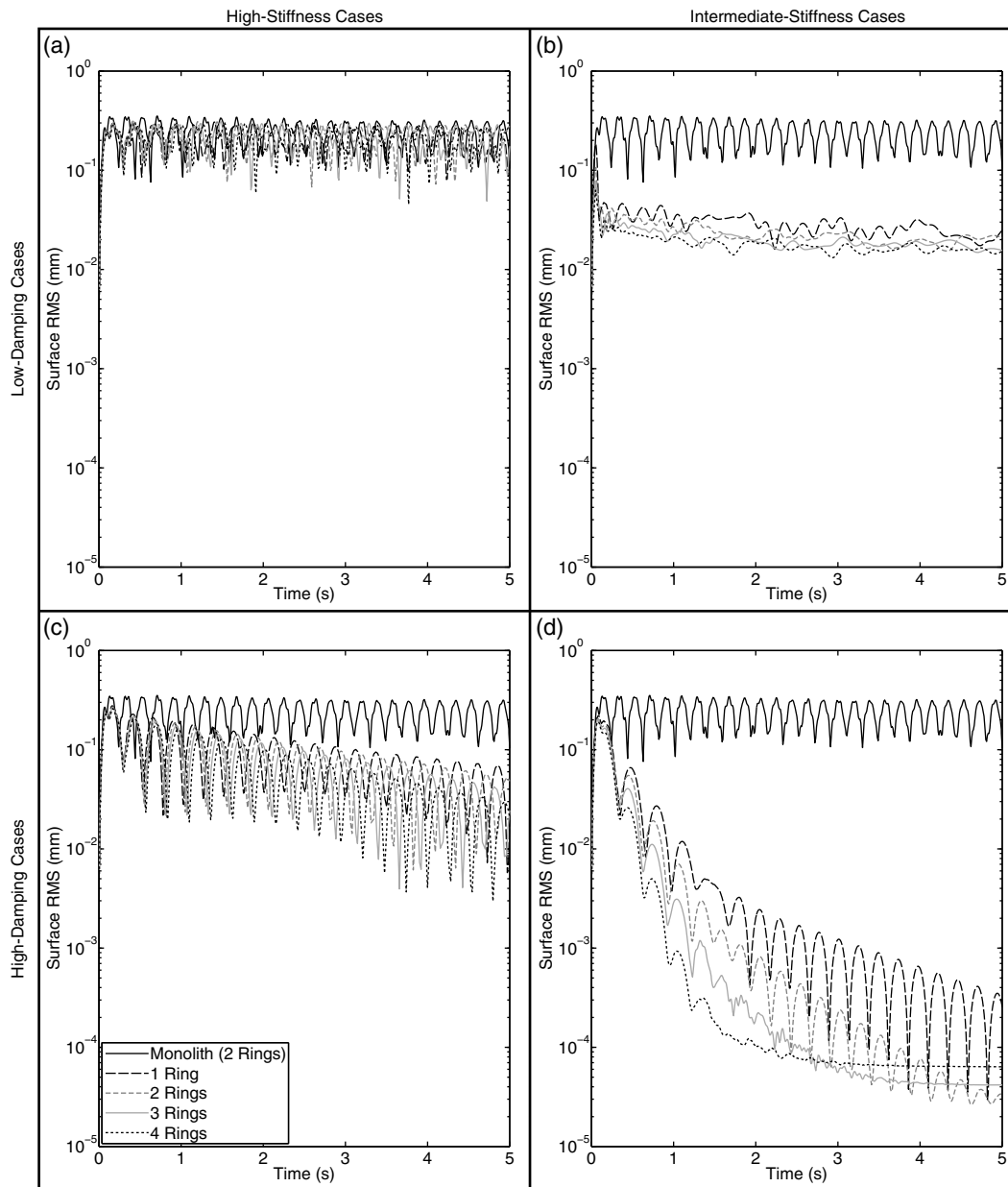


Fig. 9 The effects of ring number on the impulse response for various mechanism cases (a–d).

apparent since the segments are already connected strongly [Fig. 8(b)].

The effects of varying the ring number also depend on the mechanism stiffness. In the high-stiffness cases, the ring number primarily affects the decay rate. With low damping, the responses are all comparable to that of the monolith [Fig. 9(a)], and with high damping, the responses generally decay faster for higher ring numbers [Fig. 9(c)]. In the intermediate-stiffness cases, the ring number affects both the decay rate and the disturbance propagation. As the ring number increases, the mirror is divided into a larger number of weakly connected segments, decreasing the ease with which disturbances propagate across the mirror. As a result, the magnitude of the response decreases as the ring number increases [Fig. 9(b)]. With high damping, the responses also decay more rapidly for higher ring numbers as the decreased disturbance propagation and increased damping combine to eliminate vibration quickly [Fig. 9(d)].

While the mechanism properties and ring number all affect the final response, the selection of which parameters to increase will depend on the cost and mechanism application. Increasing the number of rings from two to three, for example, more than doubles the number of mechanisms, but the number of segments and the number of segment types double as well, adding complexity to the design. For performance comparable to a monolith, high-stiffness mechanisms must be used, and increasing the mechanism damping or ring number improves the disturbance response. For mechanisms serving as supplemental sources of stiffness and damping, increasing the ring number or mechanism damping improves the disturbance response, but excessively high damping can lead to increased disturbance propagation.

5 Summary

While increasing the primary mirror diameter presents challenges related to packaging and deployment and mirror stability,

these challenges can be addressed by using a segmented mirror architecture in which the segments are connected edgewise by mechanisms analogous to damped springs. Depending on the stiffness, these mechanisms function as either structural attachments between the segments or supplemental sources of stiffness and damping. For sufficiently high stiffnesses, the mechanisms cause the segments to move as a cohesive unit without requiring any other means of connecting the segments, such as via a backplane. In this case, the segmented mirror is dynamically comparable to a monolith, with the advantage that it can be assembled on orbit. With the additional damping provided by the mechanisms, the segmented mirror can also outperform the monolith, requiring less time to settle after vibrations are excited. For lower stiffnesses, the mechanisms may not be sufficiently strong to serve as the only connections between the segments, but the stiffness and damping contributions still improve the natural frequency and impulse response. The effects of adding a backplane are beyond the scope of this paper and may be explored in future simulations.

In general, the segmented mirror performance depends on the total stiffness and damping contributions from the mechanisms, which are affected by the individual mechanism properties as well as the total number of mechanisms. While the mechanism stiffness is primarily useful for determining the mechanism application, increasing the stiffness also increases the natural frequency and the magnitude of the impulse response. Increasing the damping generally reduces the settling time, although excessively aggressive dampers can structurally connect the segments as well. While adjusting the ring number affects the total stiffness and damping contributions, it also affects the ease with which disturbances propagate through the mirror. This effect is most noticeable if low- or intermediate-stiffness mechanisms are used since increasing the ring number divides the mirror into a larger number of weakly connected segments, decreasing the disturbance propagation. The choice of which parameters to vary to obtain the desired mirror characteristics will depend on the mechanism application and overall cost, which will be the subject of future investigation.

Acknowledgments

The authors would like to thank the NASA Graduate Student Researchers Program for its support of this project. The work was funded by NASA Grant Nos. NNX09AJ18H and NNX12AC61G.

References

1. P. A. Lightsey et al., "James Webb Space Telescope: large deployable cryogenic telescope in space," *Opt. Eng.* **51**(1), 011003 (2012).

2. Arianespace, *Ariane 5 User's Manual: Issue 5 Revision 1* (2011), http://www.arianespace.com/launch-services-ariane5/Ariane5_users_manual_Issue5_July2011.pdf.
3. M. Postman et al., "Advanced Technology Large-Aperture Space Telescope: science drivers and technology developments," *Opt. Eng.* **51**(1), 011007 (2012).
4. D. Lester et al., "Science promise and conceptual mission design for SAFIR: the Single Aperture Far-Infrared Observatory," *Proc. SPIE* **6265**, 62651X (2006).
5. H. P. Stahl et al., "Optical manufacturing and testing requirements identified by the NASA Science Instruments, Observatories, and Sensor Systems Technology Assessment," *Proc. SPIE* **8126**, 812603 (2011).
6. P. R. Lawson et al., *Terrestrial Planet Finder Interferometer (TPF-I) Whitepaper for the AAAC Exoplanet Task Force*, Jet Propulsion Laboratory, National Aeronautics and Space Administration, Pasadena, California (2007).
7. E. M. C. Kong et al., "Electromagnetic formation flight for multisatellite arrays," *J. Spacecr. Rockets* **41**(4), 659–666 (2004).
8. L. Young, *Vibrations from power supply mean more trouble for Hubble*, Baltimore Sun (7 November 1990).
9. P. Y. Bely, Ed., *The Design and Construction of Large Optical Telescopes*, Springer-Verlag, New York (2003).
10. P. Y. Bely, O. L. Lupie, and J. L. Hershey, "The line-of-sight jitter of the Hubble Space Telescope," *Proc. SPIE* **1945**, 55–61 (1993).
11. A. Danjon and A. Couder, *Lunettes et télescopes: Théorie, conditions d'emploi, description, réglage, histoire*, p. 570, Editions de la Revue d'Optique Théorique et Instrumentale, Paris (1935).
12. L. Cohan and D. W. Miller, "Launch load alleviation for lightweight, active mirrors," in *Proc. 2010 AIAA SDM Student Symposium*, American Institute of Aeronautics and Astronautics, Inc., Orlando, FL (2010).
13. M. A. Ealey, "Fully active telescope," *Proc. SPIE* **5166**, 19–26 (2004).
14. J. A. Gersh-Range et al., "A flux-pinning mechanism for segment assembly and alignment," *Proc. SPIE* **8150**, 815005 (2011).
15. H. P. Stahl, private communication (2014).
16. W. R. Arnold, Sr., *On Mirror Manufacturing Capabilities*.
17. ANSYS, Inc. *Documentation for Release 12.0.*, ANSYS, Inc., Canonsburg, PA (2009).

Jessica Gersh-Range recently completed her PhD degree in mechanical engineering at Cornell University. She was the recipient of a NASA Graduate Student Researchers Program fellowship at Marshall Space Flight Center, and she has also worked at the Space Telescope Science Institute as a graduate student. She received her BA degree in physics from Swarthmore College in 2006, with a minor in mathematics. Her research interests include space optical systems, which combines her physics and engineering backgrounds.

H. Philip Stahl is a senior optical physicist at NASA MSFC. He is leading an effort to mature technologies for a large aperture telescope to replace Hubble. Previous assignments include developing JWST mirror technology. He is a leading authority in optical metrology, optical engineering, and phase-measuring interferometry. He is a member of OSA, SPIE (fellow), and 2014 SPIE president. He earned his PhD degree in optical science at the University of Arizona, Optical Sciences Center in 1985.

Biography of the other author is not available.